Title	$D(^3He,p)^4He$ and $D(d,p)^3H$ fusion in a small plasma focus operated in a deuterium helium-3 gas mixture
Author(s)	Stuart V. Springham, Tzong H. Sim, Rajdeep S. Rawat, Paul Lee, Alin Patran, Paul M. E. Shutler, Tuck L. Tan, Sing Lee
Source	*Nukleonika, 51*(1), 47−53
Published by	De Gruyter Open

NUKLEONIKA 2006;51(1):47–53

$D(^3He,p)^4He$ and $D(d,p)^3H$ fusion in a small plasma focus operated in a deuterium helium-3 gas mixture

**Stuart V. Springham,
Tzong H. Sim,
Rajdeep S. Rawat,
Paul Lee,
Alin Patran,
Paul M. E. Shutler,
Tuck L. Tan,
Sing Lee**

Abstract A 3 kJ plasma focus was operated with a ^3He-D_2 gas mixture, with partial pressures in the ratio of 2:1, corresponding to an atomic number ratio of 1:1 for ^3He and D atoms. The fusion reactions $D(^3He,p)^4He$ and $D(d,p)^3H$ were measured simultaneously using CR-39 polymer nuclear track detectors placed inside a pinhole camera positioned on the forward plasma focus axis. A sandwich arrangement of two 1000 μm thick CR-39 detectors enabled the simultaneous registration of two groups of protons with approximate energies of 16 MeV and 3 MeV arising from the $D(^3He,p)^4He$ and $D(d,p)^3H$ reactions, respectively. Radial track density distributions were obtained from each CR-39 detector and per-shot average distributions were calculated for the two groups of protons. It is found that the $D(^3He,p)^4He$ and $D(d,p)^3H$ proton yields are of similar magnitude. Comparing the experimental distributions with results from a Monte Carlo simulation, it was deduced that the $D(^3He,p)^4He$ fusion is concentrated close to the plasma focus pinch column, while the $D(d,p)^3H$ fusion occurs relatively far from the pinch. The relative absence of $D(d,p)^3H$ fusion in the pinch is one significant reason for concluding that the $D(^3He,p)^4He$ fusion occurring in the plasma focus pinch is not thermonuclear in origin. It is argued that the bulk of the $D(^3He,p)^4He$ fusion is due to energetic $^3He^{2+}$ ions incident on a deuterium target. Possible explanations for differing spatial distributions of $D(^3He,p)^4He$ and $D(d,p)^3H$ fusion in the plasma focus are discussed.

Key words plasma focus • deuterium • helium-3 • fusion • CR-39 • track detectors

S. V. Springham✉, T. H. Sim, R. S. Rawat, P. Lee, A. Patran, P. M. E. Shutler, T. L. Tan, S. Lee
National Institute of Education,
Nanyang Technological University,
1 Nanyang Walk, Singapore 637616,
Tel.: +65 6790 3838, Fax: +65 6896 9414,
E-mail: svsprin@nie.edu.sg

Received: 25 August 2005
Accepted: 15 December 2005

Introduction

In our laboratory, plasma focus (PF) devices have been used for technological applications such as X-ray microlithography [11] as well as for fundamental studies of PF fusion [16, 17]. In the present work, we report the simultaneous measurement of two fusion reactions, $D(^3He,p)^4He$ and $D(d,p)^3H$, in a 3 kJ PF operated with a ^3He-D_2 gas mixture. (For the sake of brevity, these two reactions will be referred to here as ^3HeD and DD.) The reaction Q-values are 18.35 MeV and 4.03 MeV for ^3HeD and DD, respectively, consequently the emitted protons have very different energies: ~ 16 MeV for ^3HeD and ~ 3 MeV for DD. In the very few previously reported PF experiments performed with a ^3He-D_2 gas mixture the proton-activation of copper (via $^{63}Cu(p,n)^{63}Zn$) was used to detect the ~ 16 MeV protons [2, 6]. In the present work, the ^3HeD protons are measured directly by means of CR-39/PM-355 polymer nuclear track detectors. A pinhole camera placed on the forward axis of the plasma focus was used to image, simultaneously, the spatial distributions of the

fusion production for both the ~ 3 MeV DD protons and the ~ 16 MeV ^{3}HeD protons.

Over the years, a very large number of neutron measurements have been carried out in order to investigate deuterium fusion in the plasma focus for the reaction D(d,n)^{3}He. Characteristics of the neutron flux, such as neutron yield, energy, anisotropy, emission time and pulse shape, have been the subject of many experimental investigations [1, 18, 20]. Despite this large research effort, the fusion mechanism in the plasma focus remains poorly understood. As a means of improving theoretical models of PF fusion it must be beneficial to gather complementary experimental data for charged fusion products. To this end, measurements by Jäger *et al.* [8, 9] have demonstrated that studies of fusion protons can yield more precise results than the corresponding neutron measurements. Also, the present author has used a pinhole camera technique, with the same 3 kJ PF employed in the present work, but operated with pure deuterium gas, to image of the spatial distribution of D(d,p)^{3}H fusion protons [16]. That study concluded that 90 to 95% of the DD fusion took place in a conical region outside the PF pinch, due to beam-target interaction of energetic deuterons emitted from the pinch with the ambient deuterium filling gas.

The polymer nuclear track detector material CR-39/PM-355 (chemical formula $C_{12}H_{18}O_7$, density 1.30 g/cm^3) is well suited to charged particle measurements on the plasma focus due to its insensitivity to visible light, UV, X-rays, energetic electrons, and electromagnetic noise, all of which are emitted during the plasma focus discharge. PM-355 is a "super-grade" form of CR-39 which is reported to have the highest sensitivity to energetic light ions [19].

Plasma Focus and electrical diagnostics

The device used for these experiments was a 3 kJ UNU/ICTP plasma focus of Mather-type geometry [12]. Energy storage was provided by a single 32 μF capacitor coupled to the PF electrodes through a swinging cascade air spark-gap, and the capacitor was charged to 14 kV for all PF shots. The anode was a hollow copper tube 160 mm in length and 19 mm in diameter, with a Pyrex glass tube insulating the anode from the base plate and cathodes. The coaxial cathode comprised six copper rods arranged in a squirrel cage configuration at a radius of 3.2 cm from the PF axis. A digital oscilloscope recorded the voltage signal during the discharge via a resistive divider chain, and the dI/dt signal, where I is the electrode current measured by a Rogowski coil. The pressure of the filling gas was measured using an Edwards Barocel pressure transducer. The neutron yield per shot was measured using an activation counter comprising a paraffin moderator, and a thin indium foil coupled to a plastic scintillator and photomultiplier tube. On the forward PF axis, the proton camera was fixed to the chamber top plate. The diameter of the camera "pinhole" was 8 mm and the distance from entrance pupil to the tip of the anode was 120 mm. Within the camera the PM-355 detectors were positioned 34 mm from the entrance pupil, and the exposed area was a circle of diameter 20.4 mm. The relatively large pinhole diameter is necessitated by the observed low proton yields; consequently, the resulting pinhole image has only moderate angular resolution (~ 7° half-angle).

Design of the proton camera

For a ^{3}He-D_2 gas mixture, the energies of the emitted protons depend on the reaction mechanism. Firstly, there is a possibility of thermonuclear fusion occurring in the PF pinch, for which the emitted proton energies would be 3.0 MeV and 14.7 MeV for the DD and ^{3}HeD reactions, respectively. Secondly, beam-target fusion may occur inside or outside the pinch. Furthermore, ^{3}HeD beam-target reactions may arise from both a D^+ beam on a ^{3}He target, and a $^3He^{2+}$ beam on a D_2 target – denoted by ^{3}He(d,p)^{4}He and D(^{3}He,p)^{4}He. The ion acceleration mechanism will determine the relationship between the energies of the D^+ and $^3He^{2+}$ ions emitted from the pinch. The plasma focus ion acceleration mechanism is still not well understood theoretically, but experimental measurements have revealed its general characteristics. For many plasma devices operated in deuterium gas, the energy spectra of fast primary ions have been measured [5, 7, 17] and found to be of the form $f(E_d) \propto E_d^{-n}$, with values of n in the range of 3 to 6. There is also evidence for the existence of intense micro-sources of energetic ions [15]. We have made the simplifying assumption that an acceleration potential, V_a, of form $f(V_a) \propto V_a^{-n}$ is responsible for ion acceleration throughout the pinch column. Consequently, the $^3He^{2+}$ ions would simply have double the energy of the D^+ ions. Applying reaction kinematics, Fig. 1 shows the plots of the outgoing proton energies for beam-target ^{3}HeD and DD reactions, for incident ion energies of 60 keV (D^+) and 120 keV ($^3He^{2+}$). Since the camera is positioned on the PF forward axis we are principally concerned with forward emission angles: θ = 0° ~ 60°. From Fig. 1, it can be seen that for fusion in a ^{3}He-D_2 gas mixture,

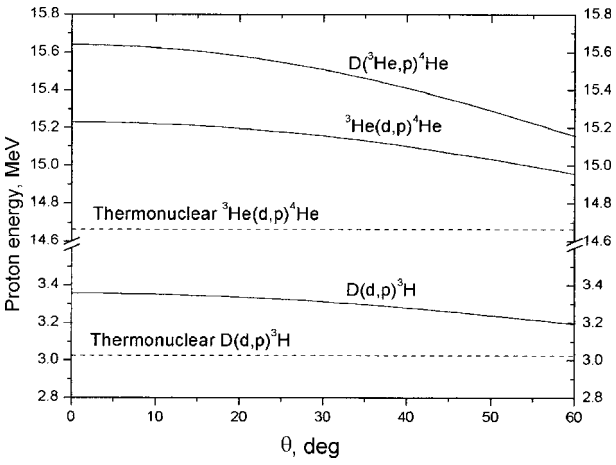

Fig. 1. Plots of proton energy as a function of emission angle θ for the fusion reactions: D(^{3}He,p)^{4}He, ^{3}He(d,p)^{4}He and D(d,p)^{3}H, for beam energies of 60 keV (D^+) and 120 keV ($^3He^{2+}$). Also shown are the outgoing proton energies for thermonuclear ^{3}He(d,p)^{4}He and D(d,p)^{3}H fusion. Note the break in the energy axis between 3.6 and 14.6 MeV.

the energy of outgoing protons can be expected to lie in two separate narrow ranges near ~ 3 MeV and ~ 16 MeV.

As a consequence of this large difference between ^{3}HeD and DD proton energy, the associated range and stopping power are also very different. The sensitivity of CR-39/PM-355 varies strongly with proton energy, and this variation can be expressed more precisely in terms of Restricted Energy Loss (REL) [4]. It is well established that the sensitivity of track detectors decreases with decreasing REL, and therefore with increasing particle energy. The track etch rate is much lower for the ~ 16 MeV ^{3}HeD protons than for the ~ 3 MeV DD protons. For the etching conditions used in these measurements we found that the PM-355 detectors were effectively insensitive to ~ 16 MeV protons. Hence, in order to detect the ^{3}HeD protons, their energy must be reduced by traversing a thick layer of material. This leads naturally to an experimental design where DD and ^{3}HeD proton tracks are measured simultaneously by a sandwich of two PM-355 detectors. The tracks for the shorter ranged DD protons are registered on the front surface of the front detector, while tracks for the longer ranged ^{3}HeD protons are registered on the back surface of the back detector.

Since ^{3}HeD and DD protons are the subject of these measurements, a 50 μm kapton filter was used to stop the other charged particles: ^{3}He (~ 0.8 MeV), ^{3}H (~ 1 MeV), ^{4}He (~ 4 MeV) and deuterons (< 2.5 MeV). SRIM Monte Carlo simulations [21] show that deuterons require energies greater than 2.5 MeV to penetrate 50 μm of kapton. The experimental results indicate that no deuterons are registered on the front PM-355 detector; hence the deuterons emitted from the PF have energies less than 2.5 MeV. The 50 μm kapton film was located at the position of the pinhole to prevent incoming primary ions producing fusion reactions within the camera. DD protons passing through this kapton film suffer an average angular deviation of 1.2°, and the deviation for the more energetic ^{3}HeD protons is significantly smaller, hence the affect of this deviation on the angular resolution of the camera is negligable. In addition, a 3 μm aluminium foil was placed between the kapton film and the front PM-355 detectors to eliminate any effect on the detectors from the visible and UV radiation emitted during the PF discharge. SRIM simulations show that normally incident 3.0 MeV protons (from DD fusion) pass through 50 μm of kapton, 3 μm of aluminium, and traverse 65 μm of PM-355 before being stopped. Taking 16.0 MeV as the upper energy limit of the ^{3}HeD protons, the corresponding path length in PM-355 is 2.220 μm (after passage through the kapton and aluminium filters). Moreover, the specific energy loss of the protons at the front PM-355 surface is much lower for the ^{3}HeD protons (5 keV/μm) than for the DD protons (20 keV/μm); this difference explains the insensitivity of PM-355 detectors to full energy ^{3}HeD protons. From a number of SRIM simulations and the results of preliminary investigations reported below, it was decided that the optimum detector arrangement was two PM-355 detectors each of 1000 μm thickness placed after the 50 μm kapton and 3 μm aluminium

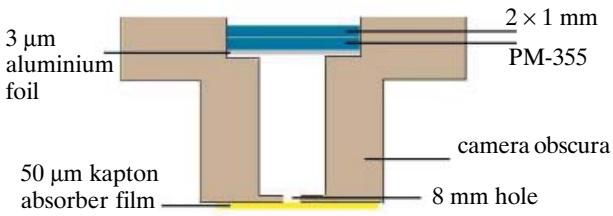

Fig. 2. Schematic diagram of the proton camera showing the positions of the PM-355 detectors, and the aluminium and kapton filters.

filters. A schematic diagram showing the arrangement of the proton camera, filters and detectors is given in Fig. 2. With this arrangement only DD protons are registered on the forward-most PM-355 surface, while only ^{3}HeD protons are registered on back-most surface. At the interface of the two PM-355 detectors, SRIM simulations indicate that the ^{3}HeD protons will have energies of approximately 11 MeV. Etched tracks are generally not observed at these mid-depth surfaces.

Experimental procedure

Deuterium and ^{3}He gases were mixed in the PF chamber with partial pressures in the ratio of 1:2, corresponding to an atomic number ratio of 1:1 for D and ^{3}He atoms. Precise mixing was ensured by means of a pressure transducer with a precision of ~ 10^{-2} mbar. Operation of the PF device was tested for a range of total pressures ranging from 4.2 mbar to 6.0 mbar. A total gas pressure of 4.8 mbar (3.2 mbar of ^{3}He gas plus 1.6 mbar of D_2 gas) was chosen for the main experimental work. This total pressure was selected on the basis that it gave a suitable plasma sheath rundown time (~ 1/4 discharge period), sharp peaks in the dI/dt trace, and reasonable neutron yield as measured by the indium activation counter.

Several preliminary experiments were performed with the aim of determining the optimum thickness for the PM-355 detectors for separate registration of DD and ^{3}HeD protons with high efficiency. Multilayer stacks of PM-355 plates with various thickness combinations were exposed inside the camera; the individual plate thicknesses used were 250, 500 and 1000 μm. The 50 μm kapton and 3 μm aluminium filters were used throughout. After exposure, the same etching procedure was used for all detectors: 6.25 M NaOH solution at 70°C for 24 hours. Figure 3 shows a microscope image obtained from one PM-355 detector for a stack comprising: 50 μm kapton + 3 μm Al + (1000 + 250 + 250 + 250 + 250) μm PM-355. Visual examination of many such detectors led us to the conclusion that separate registration of DD and ^{3}HeD protons, with high efficiency, was best achieved using two PM-355 detectors of 1000 μm thickness, and this is the arrangement adopted for the subsequent experimental measurements.

For the main experimental work, 5 detector pairs were exposed to a total of 119 plasma focus shots: averaging approximately 24 shots per detector-pair. The arrangement of the camera and PM-355 detectors

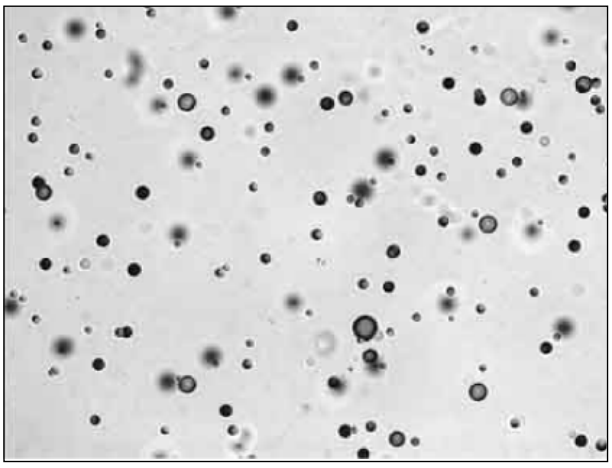

Fig. 3. Photomicrograph of an initially 250 μm PM-355 plate (less than 200 μm thick after etching) from a multilayer stack. Etched tracks, due to the passage of ^{3}HeD protons, are visible on both the in-focus and out-of-focus surfaces. The pictured detector plate was posterior to PM-355 plates with a cumulative thickness 1500 μm.

was as shown in Fig. 2. The same etching procedure was applied to both front and back PM-355 detectors: 6.25 M NaOH solution at 70°C for 24 hours. After etching the detectors were scanned using an automated system [16]. Spurious tracks were eliminated from the analysis by applying shape, size and grey-value criteria to the dark features recognised and measured by the automated scanning system. Figure 4 shows a digital photograph of a front PM-355 detector after etching. The circular pattern of tracks due to DD protons can be clearly seen.

For the purpose of comparison, the same camera geometry was used with pure D_2 as the plasma focus filling gas at a pressure of 4.0 mbar. For pure deuterium, the DD yield is much higher than for the ^{3}He-D_2 gas mixture, and a single PF shot was sufficient to expose a PM-355 detector. Thirteen PM-355 detectors were exposed to one shot each. Since only DD reactions can occur, a single 1000 μm PM-355 layer was used for these exposures.

Fig. 4. Macro photograph image of a front 1000 μm PM-355 plate showing the exposure pattern for DD proton etched tracks. The diameter of exposed circle is 20.4 mm.

Results and discussion

The track information extracted from the PM-355 detectors by the automated scanning system was analysed in a similar manner to that described in Ref. [16]. Radial track density distributions were obtained for each detector, with concentric 0.5 mm annular rings representing the bins for the distribution: resulting in 20 radial bins. The distributions for the five front detectors were summed and divided by the total number of PF shots (= 119) to give a per-shot average distribution for the ~ 3 MeV DD protons; the same procedure was applied to the five back detectors giving a corresponding distribution for the ~ 15 to ~ 16 MeV ^{3}HeD protons. Plots of these distributions are shown in Fig. 5. A very pronounced central peak is apparent in the ^{3}HeD distribution. By contrast to the DD distribution displays a very shallow and slightly broader central peak, being quite flat out to a radius of ~ 5 mm. From the pinhole camera principle, it can be inferred that the ^{3}HeD fusion occurs predominantly close to (or inside) the pinch column, whereas the DD fusion is much more widely distributed in space. Furthermore, the number of proton tracks on the front and back detectors are found to be very similar: the 5 front detectors (DD protons) having a total of 67,500 tracks, while the 5 back detectors have 66,400 tracks (rounded to the hundreds). Hence, notwithstanding the different spatial distributions associated with the ^{3}HeD and DD fusion, it is apparent that the total proton yields for the ^{3}HeD and DD reactions are similar.

With regard to the fusion mechanisms involved, the possibility of thermonuclear fusion in the pinch can be

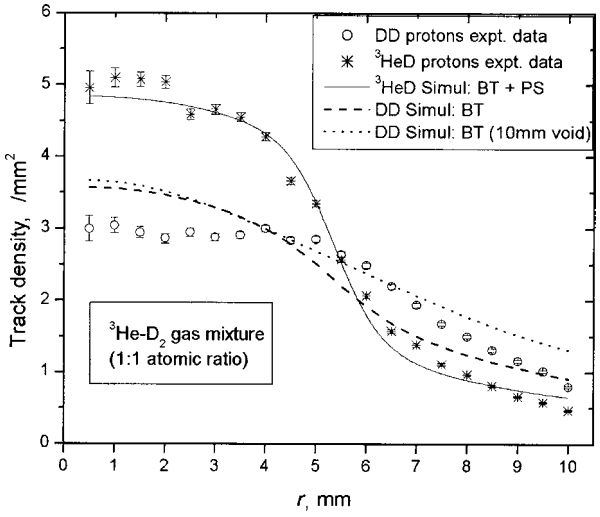

Fig. 5. Plot of radial track density distributions for the front and back PM-355 detectors: DD and ^{3}HeD protons, respectively (^{3}He-D_2 filling gas). Distributions are per-shot averages from 5 front and 5 back detectors. The acronyms BT and PS refer to beam-target and pinch-source, respectively. The curves shown are discussed in the text.

examined first. From Ref. [13], it can be seen that the ^{3}HeD rate falls rapidly for plasma temperatures below ~ 20 keV. At 4 keV, for a given plasma density, the ^{3}HeD rate is more than an order of magnitude lower than the DD rate. Time and space resolved X-ray measurements [14] indicate that when neutron emission begins in the plasma focus, the pinch temperature is ~ 1 keV. Assuming that the atomic number density of D and ^{3}He ions in the pinch column is 1:1 (as it is in the ambient gas), then the DD thermonuclear yield should be many times greater than the ^{3}HeD thermonuclear yield. However, the data presented in Fig. 5 shows that, in contradiction with the thermonuclear model, there are considerably more ^{3}HeD protons than DD protons being emitted from the region of the pinch column. It can be concluded, therefore, that the ^{3}HeD fusion occurring in the pinch region is due to beam-target interactions. This does not exclude the possibility that the DD fusion is also beam-target in nature.

In order to make a meaningful comparison between the ^{3}HeD and DD proton yields in terms of the beam-target model, we must examine the reaction cross sections. An empirical approximation [3] has been used to compute the cross sections shown in Fig. 6, and these computed cross sections are found to be in good agreement with the experimental data of Krauss *et al.* [10]. Note that the cross sections are plotted in terms of the notional acceleration potential: V_a. For example, for V_a = 50 kV, the D^+ and $^3He^{2+}$ have lab kinetic energies of 50 keV and 100 keV, respectively. It can be seen that the cross section for D(^{3}He,p)^{4}He is significantly larger than that for ^{3}He(d,p)^{4}He for all values of V_a. Since the PF gas mixture contains a D and ^{3}He atomic ratio of 1:1 (and assuming the ratio of D^+ and $^3He^{2+}$ beam ions is similarly 1:1), then the bulk of ^{3}HeD beam-target fusion should result from the D(^{3}He,p)^{4}He reaction. Moreover, the very similar ^{3}HeD and DD proton yields observed suggests that the D(^{3}He,p)^{4}He and D(d,p)^{3}H reaction cross sections are also of similar magnitude. If the above arguments are valid, then from Fig. 6 it is possible to roughly estimate the beam energies as 55 keV for the D^+ ions and 110 keV for the $^3He^{2+}$ ions.

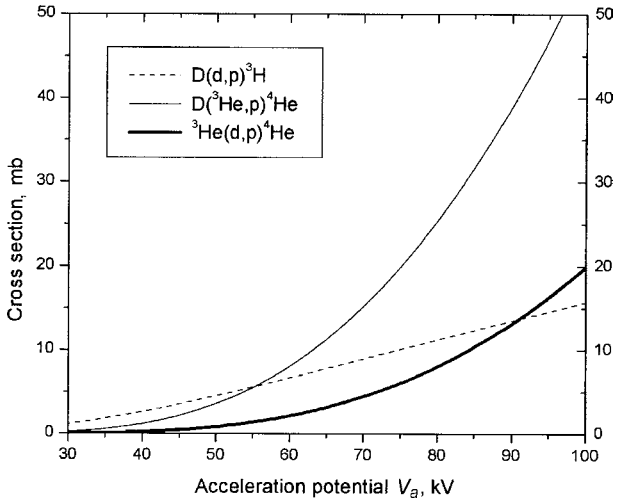

Fig. 6. Plots of cross section as a function of accelerating potential V_a for the fusion reactions: D(d,p)^{3}H, D(^{3}He,p)^{4}He and ^{3}He(d,p)^{4}He.

It is interesting to compare the DD proton distribution for the ^{3}He-D_2 gas mixture (Fig. 5) with the corresponding distribution for pure D_2 gas (Fig. 7). The total number of protons tracks recognized was 173,400 (rounded to the hundreds). Two points are immediately apparent: (i) the average yield of DD protons is much lower (about a factor of about 30) when the PF is operated with a ^{3}He-D_2 gas mixture than for pure D_2 gas, and (ii) the shape of the DD distribution is much shallower for the ^{3}He-D_2 gas mixture than the pure D_2 case.

Considering the first point, the simplest fusion models would predict a factor of 4 reduction in DD proton yield for the ^{3}He-D_2 mixture as compared with pure D_2 gas. This prediction is based on a factor of 2 reduction in the deuteron density in the hot pinch plasma, the cold ambient gas, and the number of energetic deuterons in the beam; all other factors being equal (pinch temperature, ejected ion energies, etc.). The fact that the DD proton yield is reduced by a much larger factor (approximately 30) is likely to indicate that the fundamental mechanisms occurring in the pinched plasma (compression, heating, ion acceleration, etc.) are qualitatively different vis-à-vis the pure D_2 and ^{3}He-D_2 cases.

With regard to the second point, the solid curve plotted in Fig. 7 shows that the pure deuterium distribution can be well fitted by a linear combination of beam-target and pinch-source contributions calculated from a Monte Carlo simulation code PF-Moca [16]. This fit corresponds to a 91% contribution from beam-target (BT) fusion (50 keV deuterons emitted from pinch in a cone of half-angle 60°), plus a 9% pinch-source (PS) contribution. The pinch-source protons are assumed to be emitted isotropically. However, for the DD distribu-

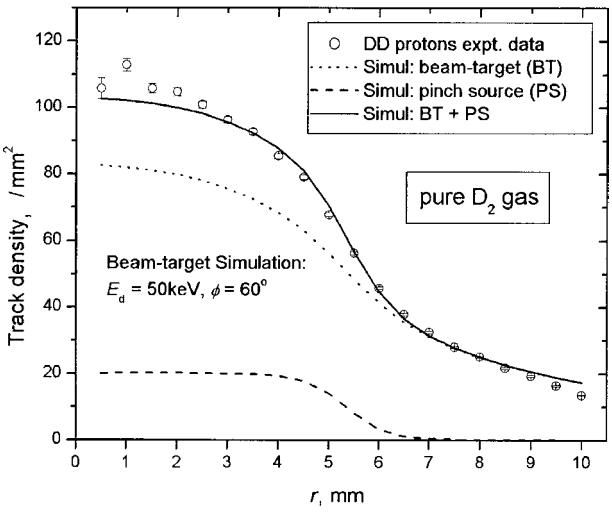

Fig. 7. Plot of radial track density distribution for the DD protons obtained for 12 PF shots (one PM-355 detector exposed per shot) using pure D_2 as the filling gas. Distributions are per-shot averages. The curves shown are results from the plasma focus Monte Carlo simulation, PF-Moca, with: 91% contribution from beam-target fusion (50 keV deuterons emitted from pinch in a cone of half-angle 60°), plus a 9% pinch source contribution.

tion associated with the ^{3}He-D_2 gas mixture, a satisfactory fit with PF-Moca simulation cannot be obtained due to the shallowness of the experimental distribution. As can be seen from Fig. 7, the central peaking of the DD distribution is partly due to the pinch-source contribution. Eliminating the pinch-source contribution entirely, and considering only beam-target fusion, the PF-Moca generated distribution is still not as shallow as the experimental DD distribution. The PF-Moca simulation program uses the (lab frame) differential cross section for the D(d,p)^{3}H reaction (which is quite anisotropic), as well as the stopping power for the deuterons traversing the filling gas – both of these effects contributing to the central peaking of the simulated DD distribution. However, even if the simulation is performed using the (incorrect) assumptions that: (i) the D(d,p)^{3}H reaction is entirely isotropic in the lab frame, and (ii) the stopping power for deuterons traversing the gas is zero – the central peaking of the simulated distribution is reduced, but it is still not as shallow as the DD experimental data. Such a "flattened" distribution is plotted (dashed line) in Fig. 5 (cone half-angle $\phi = 60°$), normalised so as to pass through the $r = 4$ mm data point; the shallowness of the experimentally observed distribution is clearly not reproduced. One additional PF-Moca simulation curve is shown in Fig. 5 (dotted line), also normalised at $r = 4$ mm. This curve is generated using the ad hoc assumption of a spherical void (radius 10 mm) centred on the pinch, in which no DD fusion occurs. Beyond the void beam-target fusion still occurs in a cone of half-angle $\phi = 60°$. This ad hoc assumption moves the fusion further from the pinch column and produces a shallower distribution; however, it still fails to reproduce the observed distribution.

Conclusions

For a 3 kJ plasma focus operated in a ^{3}He-D_2 gas mixture (1:1 atomic ratio), DD and ^{3}HeD proton tracks are measured simultaneously by a sandwich of two PM-355 detectors, and the associated regions of fusion production are imaged by means of a pinhole camera arrangement. In view of the paucity of existing experimental results for He-D_2 gas mixtures, the present work represents a significant addition to the published data. Moreover, the $\sim$ 16 MeV ^{3}HeD protons are observed directly using polymer nuclear track detectors, in contrast to previous studies which employed the proton-activation of copper.

The overall proton yields for the ^{3}HeD and DD reactions are found to be similar. The ^{3}HeD distribution is observed to be centrally peaked, and this distribution can be well fitted with PF-Moca simulations for which the pinch-source contribution is in the range of 20 to 30% of the total D(^{3}He,p)^{4}He yield. It does not seem possible to explain this substantial quantity of ^{3}HeD fusion occurring in the PF pinch in terms of thermonuclear fusion, as this would require significantly higher pinch temperatures than have been reported previously. Moreover, the presence of such high temperature D^+ ions (necessary for thermonuclear ^{3}HeD fusion) would give rise to a large DD thermonuclear yield. However, contradicting this expectation, the experimental distribution for DD protons shows a notable absence of DD fusion in the PF pinch.

The shallowness of the observed DD distribution is one aspect of the experimental data which is particularly difficult to explain. In general terms, this shallowness indicates that the DD fusion is occurring relatively far from the pinch. Even the introduction of the ad hoc assumption of a spherical "DD fusion void" centred on the pinch, in combination with the incorrect assumptions of isotropic proton emission and zero stopping power for deuterons in the filling gas, does not permit a satisfactory fit to the experimental data to be obtained with the PF-Moca simulation. In addition, a series of exposures performed with pure D_2 gas yields a DD distribution which is quite dissimilar to the DD distribution found for the ^{3}He-D_2 mixture. The pure D_2 distribution displays a much more "normal" shape, and can be satisfactorily fitted using the PF-Moca code. One possible explanation for the observed shallowness of the ^{3}He-D_2 DD data is that energetic D^+ ions are emitted from the plasma focus pinch in predominantly radial directions: $\theta > 45°$. These deuterons would then pass through the low ion density region behind the plasma current sheath, before passing through the sheath into the ambient gas where they would produce beam-target fusion – this would result in an annular ring of DD emission around the PF pinch. The centrally peaked ^{3}HeD is explicable in terms of $^3He^{2+}$ ions being accelerated in axial directions, producing beam-target fusion within the pinch and in a forwardly directed cone ahead of the pinch. It should be remembered that the radial distributions obtained are averages over a large number of shots, so it may be the case that for any given shot the ions accelerated (in different directions) are predominantly D^+ ions or $^3He^{2+}$ ions. An understanding of why the D^+ and $^3He^{2+}$ ions would be emitted in different directions would probably require more detailed theoretical models of the plasma focus radial compression phase, and the of ion acceleration mechanism, than are presently available.

Acknowledgment The authors are pleased to acknowledge the financial support for this work provided by the International Atomic Energy Agency (CRP contract No. 12412), and the National Institute of Education, Nanyang Technological University, Singapore (grant No. RI 2/04 SVS).

References

1. Bernard A, Coudeville A, Jolas A, Launspach J, de Mascureau J (1975) Experimental studies of the plasma focus and evidence for nonthermal processes. Phys Fluids 18:180–194
2. Brzosko JS, Nardi V, Brzosko JR, Goldstein D (1994) Observation of plasma domains with fast ions and enhanced fusion in plasma-focus discharges. Phys Lett A 192:250–257
3. Duane BH (1972) Fusion cross section theory. BNWL-1685, Brookhaven National Laboratory
4. Durrani SA, Bull RK (1987) Solid state nuclear track detection. Pergamon Press, New York

5. Gerdin G, Stygar W, Venneri F (1981) Faraday cup analysis of ion beams produced by a dense plasma focus. J Appl Phys 52:3269–3275
6. Gullickson RL, Luce JS, Sahlin HL (1977) Operation of a plasma-focus device with D_2 and ^{3}He. J Appl Phys 48:3718–3722
7. Gullickson RL, Sahlin HL (1978) Measurements of high-energy deuterons in the plasma-focus device. J Appl Phys 49:1099–1105
8. Jäger U, Bertalot L, Herold H (1985) Energy spectra and space resolved measurements of fusion reaction protons from plasma focus devices. Rev Sci Instrum 56:77–80
9. Jäger U, Herold H (1987) Fast ion kinetics and fusion reaction mechanism in the plasma focus. Nucl Fusion 27;3:407–423
10. Krauss A, Becker HW, Trautvetter HP, Rolfs C, Brand K (1987) Low-energy fusion cross section of D+D and D+^{3}He reactions. Nucl Phys A 465:150–172
11. Lee S, Lee P, Zhang G *et al*. (1998) Powerful soft X-ray sources and high resolution lithography. Sing J Phys 14:1–9
12. Lee S, Tou TY, Moo SP *et al*. (1988) A simple facility for the teaching of plasma dynamics and plasma nuclear fusion. Am J Phys 56:62–68
13. Lilley JS (2001) Nuclear physics: Principles and applications. Wiley, New York, p 303
14. Rout RK, Shyam A (1989) Observation of helical structures in a low energy plasma focus pinch. Plasma Phys Controlled Fusion 31:873–877
15. Sadowski M, Składnik-Sadowska E, Baranowski J (2000) Comparison of characteristics of pulsed ion beams emitted from different small PF devices. Nukleonika 45;3:179–184
16. Springham SV, Lee S, Moo SP (2002) Deuterium plasma focus measurements using solid state nuclear track detectors. Braz J Phys 32:172–178
17. Springham SV, Lee S, Rafique MS (2000) Correlated deuteron energy spectra and neutron yield for a 3 kJ plasma focus. Plasma Phys Controlled Fusion 42:1023–1032
18. Steinmetz K, Hubner K, Rager JP, Robouch BV (1982) Neutron pinhole camera investigation on temporal and spatial structures of plasma focus neutron source. Nucl Fusion 22:25–29
19. Szydłowski A, Sadowski M, Czyżewski T, Jaskóla M, Korman A (1999) Comparison of responses of CR-39, PM-355, and PM-600 track detectors to low-energy hydrogen, and helium ions. Nucl Instrum Meth B 149:113–118
20. Tiseanu I, Mandache N, Zambreanu V (1994) Energetic and angular characteristics of the reacting deuterons in a plasma focus. Plasma Phys Controlled Fusion 36:417–432
21. Ziegler JF, Manoyan JM (1988) The stopping of ions in compounds. Nucl Instrum Meth B 35:215–228